JACS
JOURNAL OF THE AMERICAN CHEMICAL SOCIETY
Article
pubs.acs.org/JACS

Two-Dimensional Chirality Transfer via On-Surface Reaction

Haiming Zhang,[†] Zhongmiao Gong,[†] Kewei Sun,[†] Ruomeng Duan,[‡] Penghui Ji,[†] Ling Li,[†] Chen Li,[‡] Klaus Müllen,[‡,§] and Lifeng Chi*[,†]

[†]Institute of Functional Nano&Soft Materials (FUNSOM), Jiangsu Key Laboratory for Carbon-Based Functional Materials & Devices, Soochow University, 199 Ren'ai Road, Suzhou, Jiangsu 215123, People's Republic of China

[‡]Max Planck Institute for Polymer Research, Ackermannweg 10, D-55128 Mainz, Germany

[§]Institute of Physical Chemistry, Johannes Gutenberg University Mainz, Duesbergweg 10-14, D-55128 Mainz, Germany

Supporting Information

ABSTRACT: Two-dimensional chirality transfer from self-assembled (SA) molecules to covalently bonded products was achieved via on-surface synthesis on Au(111) substrates by choosing 1,4-dibromo-2,5-didodecylbenzene (12DB) and 1,4-dibromo-2,5-ditridecylbenzene (13DB) as designed precursors. Scanning tunneling microscopy investigations reveal that their aryl−aryl coupling reaction occurs by connecting the nearest neighboring precursors and thus preserving the SA lamellar structure. The SA structures of 12(13)DB precursors determine the final structures of produced oligo-*p*-phenylenes (OPP) on the surface. Pure homochiral domains (12DB) give rise to homochiral domains of OPP, whereas lamellae containing mixed chiral geometry of the precursor (13DB) results in the formation of racemic lamellae of OPP.

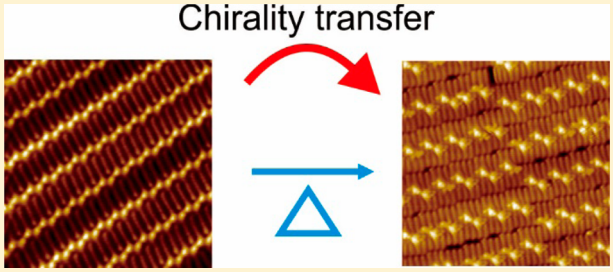

INTRODUCTION

Chiral synthesis and separation are particularly important in the pharmaceutical industry because of the demand for pure enantiomers.[1−3] Since solid surfaces are essential for basic physical and chemical processes, such as adsorption, self-assembly, and catalysis, on-surface chirality has become a significant issue in this active research field. Thanks to the invention of scanning tunneling microscopy (STM), on-surface chirality has been intensively explored at a molecular scale in recent decades.[4−7] It has been realized that the adsorption of molecules, regardless of their chiral,[8−10] prochiral,[11−14] or achiral structure,[15−17] can give rise to a chiral packing structure on surfaces. Although most of the two-dimensional (2D) chiral structures prepared on single-crystal surfaces are overall 2D racemates, on-surface homochirality can be obtained by introducing a small amount of guest chiral molecules to the self-assembled monolayers (SAMs)[18,19] or using a chiral solvent at the liquid/substrate interface.[20] However, because the forces governing such an on-surface chiral packing are mainly noncovalent, for example, via hydrogen bonding, van der Waals interactions, as well as metal−organic coordination, the low stability of the resulting chiral structures limits their practical applications in chiral synthesis and separation.

Recent developments toward on-surface synthesis, on the other hand, establish a way to fabricate thermally stable 1D and 2D covalently connected structures on surfaces.[21−23] Initiated by thermal annealing or ultraviolet (UV) irradiation, precursor molecules with functional groups, such as halides,[21,24,25] alkynes,[26,27] and boronic acids,[28,29] can be activated to produce radicals on surfaces after the dissociation of chemical bonds. Typically, the radicals will connect with substrate atoms to form metal−organic hybrids as an intermediate state and finally give rise to thermally stable 1D and 2D structures by reverting metal atoms to the substrate.[25,30,31] To date, considerable achievements have been made in this area, as exemplified by the synthesis of graphene nanoribbons with atomic precision.[32−34] However, little research has been directed toward the synthesis of chiral structures on surfaces, partially because the connection of radicals on surfaces often proceeds in a random and uncontrollable fashion. One work was reported by De Schryver et al., where self-assembled domains of alkylated diacetylenes can be partially polymerized at the liquid/substrate interface under the exposure of a UV lamp.[35] In this case, the chirality of the domains can be preserved after photopolymerization. Because the reaction is limited to molecules with reactive diacetylenes, a more general method is required, specifically concerning the synthesis of functional chiral materials, such as chiral graphene nanoribbons. Taking into account the role of noncovalent interactions in directing chiral self-assembly on surfaces, we report here the successful 2D chirality transfer from self-assembled molecules to covalently connected oligomers via aryl−aryl coupling reactions on Au(111) under the assistance of noncovalent interactions. Chirality expression of produced oligomers is determined by the packing structures of self-assembled monolayers so that it can also be controlled by adjusting self-assembled structures. The crucial role of

Received: June 1, 2016
Published: August 22, 2016

DOI: 10.1021/jacs.6b05597
J. Am. Chem. Soc. 2016, 138, 11743−11748

noncovalent adsorbate−substrate interactions in chirality transfer from chiral SAMs to chiral oligomers will be highlighted.

RESULTS AND DISCUSSION

1,4-Dibromo-2,5-didodecylbenzene (12DB) and 1,4-dibromo-2,5-ditridecylbenzene (13DB) are used as precursor molecules based on the following considerations: two alkyl chains can provide sufficient molecule−molecule interaction to direct the self-assembly of molecules on the Au(111) surface, and two bromo substituents offer potential sites for homolytic radical formation and subsequent carbon−carbon connections. The existence of alkyl chains breaks the mirror plane (σ_v) of 1,4-dibromobenzene, leading to possible enantiomers upon adsorption of the precursors on surfaces. Different alkyl chains with even (12DB) and odd (13DB) carbon numbers are adopted to investigate the role of noncovalent interactions in chirality transfer of produced oligomers, that is, oligo-*p*-phenylenes (OPP). Shown in Figure 1a is a typical STM image of 12DB SAMs prepared by evaporating 12DB on the Au(111) substrate held at room temperature (RT) under ultrahigh vacuum conditions. 12DB molecules self-assemble on the Au(111) surface to form a well-ordered lamellar structure, a characteristic feature of the SAMs of alkane derivatives.[12,17] The unit cell parameters are $a = 2.11 \pm 0.02$ nm and $b = 1.01 \pm 0.02$ nm. Two bright bumps observed in the middle of the molecule represent the position of bromo substituents. Alkyl chains of the 12DB molecule are found to adsorb along the $[1\bar{1}0]$ direction. The intermolecular distance between alkyl chains is 0.5 nm, which is consistent with the periodic distance of gold atoms along the $[11\bar{2}]$ direction. Since the adsorption of 12DB on the Au(111) surface breaks the mirror plane (σ_h) of the molecule (C_{2h} point group with a mirror plane parallel to the benzene plane), chiral packing structures are observed in the SAMs of 12DB, as depicted in Figure 1b. Two adjacent homochiral domains, marked as "R" and "S", are connected to form an angle of 30° between the long axis of each unit cell. Detailed structures of each homochiral domain are collected in high-resolution STM images, as depicted in Figure 1c. The enantiomeric packing of 12DB can be easily recognized from atomic resolution STM images and is more clearly displayed in a structural model (see Figure 1d).

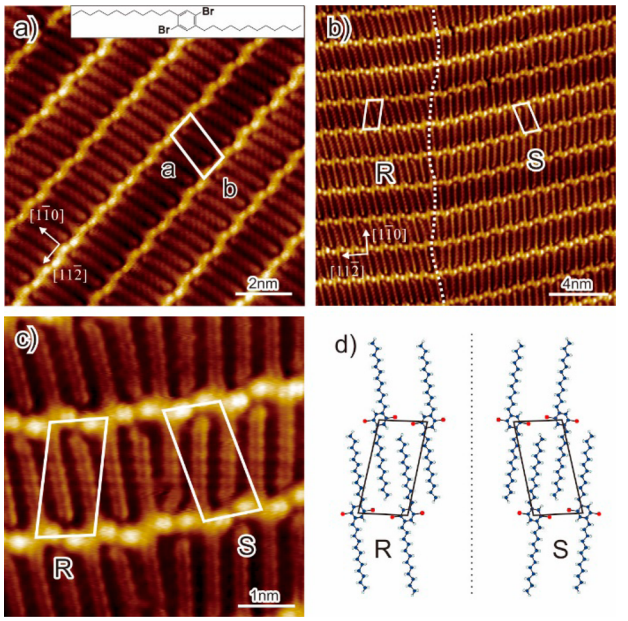

Figure 1. (a) Self-assembled monolayers of 12DB on the reconstructed Au(111). (b) STM image of the chiral packing structures in the SAMs of 12DB. The dotted line highlights the boundary between two homochiral domains of "R" and "S". (c) High-resolution STM image of the boundary between "R" and "S" domains, showing detailed molecular packing of each domain. (d) Structural model describing the packing of 12DB to form chiral structures on surface.

To investigate the chirality transfer from molecular packing of 12DB to the chains of OPP, the Au(111) substrate covered by ca. 0.5 monolayer (ML) 12DB was annealed at 100 °C for breaking C−Br bonds and achieving aryl−aryl coupling. The STM image (Figure 2a) depicts the beginning of a series of such bond-forming processes. While the overall structure of the 12DB SAMs is maintained (e.g., unchanged distance between lamellae), the appearance of dark spots (marked by white arrows in Figure 2a) in the SAMs reflects the preliminary stage of the coupling reaction. The origin of the dark spot can be attributed to the formation of a new entity, which is composed of four alkyl chains and one central core, as marked by a dashed outline in Figure 2a. Since each 12DB loses one bromo substituent and the distance (1.05 ± 0.02 nm) between two bright bumps of the central core is in line with the distance between bromo substituents of a 12DB dimer, we assign the new entity to the 12DB "dimer", as displayed in Figure 2a. It is therefore a reasonable assumption that the dark spot is formed by squeezing out adjacent 12DB molecules by connecting 12DB in the same lamella. Further annealing of the sample at 120 °C for 5 min leads to additional reactions within the SAMs on Au(111), in which no single 12DB molecule is observable anymore. Homochiral islands of 12DB oligomers, marked as "R" and "S", can be clearly recognized from the STM image, as shown in Figure 2b. The alkyl chains of 12DB "oligomers" are

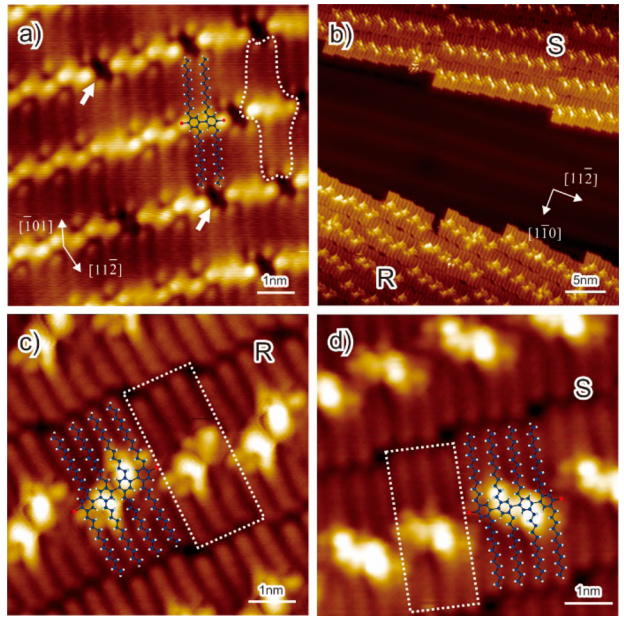

Figure 2. Chirality transfer from 12DB molecules to oligomers. (a) STM image of the sample annealed at 100 °C, showing the coexistence of intact 12DB molecules and "dimers". (b) STM image of homochiral islands of 12DB oligomers, highlighted as "R" and "S". Detailed structures of each homochiral island are collected in high-resolution STM image of "R" (c) and "S" (d) islands.

DOI: 10.1021/jacs.6b05597
J. Am. Chem. Soc. 2016, 138, 11743−11748

adsorbed along the [1$\bar{1}$0] direction, similar to that of a single 12DB molecule adsorbed on the Au(111). A closer view at each homochiral island reveals detailed structure of 12DB oligomers, as displayed in Figure 2c,d. The SAMs of 12DB oligomers are mainly composed of 12DB "tetramers", but a few "trimers", highlighted by a white rectangle, are still observable in the SAMs. Alkyl chain segments close to phenylene moieties exhibit enhanced tunneling probability in the STM image, which can be attributed to the slight twisting of adjacent phenylene moieties due to steric effects. Annealing at a higher temperature (ca. 160 °C) can give rise to longer oligomer chains on Au(111) (see Supporting Information, Figure S1). However, because of the complicated twisting structure of phenylene moieties in the longer chains, chirality assignment of each chain becomes difficult from STM images.

To further verify the covalently connected OPP structures, we used scanning tunneling spectroscopy (STS) to investigate the different electronic structures of 12DB "trimer" and "tetramer". STS measurements of the oligophenylenes have been performed on several samples with various tips. Shown in Figure 3a is typical dI/dV spectra recorded with the STM tip

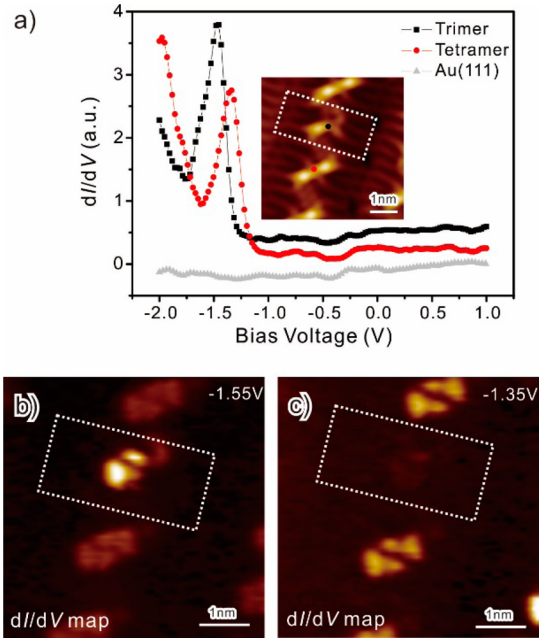

Figure 3. STS measurement of the 12DB oligomers. (a) Typical dI/dV spectra recorded on bare Au(111) (gray), 12DB trimer (black), and tetramer (red). Both dI/dV spectra of 12DB oligomers are offset vertically for a better view. Spatial distributions of electronic structure in dI/dV mappings obtained respectively at V_{bias} = −1.55 V (b) and −1.35 V (c) exhibit remarkable difference of 12DB trimer and tetramer.

on top of the center of the 12DB trimer (black) and tetramer (red), as indicated by a black and a red spot in the inset of Figure 3a. To ensure the reliability of STS data, a spectrum on bare Au(111) (gray) with the same tip is recorded as a reference before each measurement. Both dI/dV curves are featureless over the range measured in the empty states ($0 < V_{bias} < 1$), whereas a remarkable difference in the filled states is detectable. The resonant state of the 12DB trimer (black curve) at V_{bias} = −1.5 V is 0.15 V negative from that obtained on top of 12DB tetramer (red curve, −1.35 V). Such a difference in dI/dV curves is more evident in the spatial distribution of electronic structures, which is recorded by constant bias dI/dV mapping at a sample bias near the resonant state of 12DB trimer (−1.55 V, Figure 3b) and tetramer (−1.35 V, Figure 3c). The enhanced intensity is only observed in the central part of oligophenylenes, which is consistent with the fact that the frontier orbitals of OPP are mainly distributed around the phenylene moieties.[36] The dI/dV intensity of 12DB trimer (highlighted by a white rectangle) in the central part is significantly weakened when the sample bias is shifted from −1.55 V (Figure 3b) to −1.35 V (Figure 3c). The red shift of the resonant state from the 12DB trimer to tetramer corresponds well with previous experimental results that the highest occupied state of OPP will decrease with increasing length of the phenylene moieties.[36] STS measurements can thus further confirm the structure of oligo-*p*-phenylenes.

In general, chirality transfer from self-assembled precursors to oligomers via on-surface synthesis is difficult to achieve, as newly formed covalent bonds between molecules can significantly decrease intermolecular distance and thus determine the final structure of products. The latter, however, is normally different from the original molecular packing in SAMs. In consideration of the intermediate state during on-surface reactions, the structural similarity of SAMs and produced oligomers or polymers becomes more difficult in practice. In the remarkable case of chirality transfer of 12DB, molecules are fully confined in the lamellae and can only be coupled with the nearest neighboring molecules by squeezing out the next-nearest neighboring molecules, as the rotation and the flip of molecules are restricted by lateral interactions of alkyl chains. With the assistance of parallel packed alkyl chains, on-surface coupling reactions of 12DB can proceed in a controllable way, thus allowing the chirality transfer and also chiral amplification from the self-assembled molecules to the linear oligomers.

To further demonstrate the correlation between structures of SAMs and oligomers, another precursor molecule 13DB was adopted. The SAMs of 13DB were prepared on Au(111) surface held at RT in the similar way as for 12DB. Shown in Figure 4a is an STM image of the 13DB SAMs, in which parameters of the unit cell are $a = 2.23 \pm 0.02$ nm and $b = 0.99 \pm 0.02$ nm. While the lamellar structure of 13DB is similar to that of 12DB, careful inspection indicates that no homochiral domains exist. In the "R"-dominated domain, as displayed in Figure 4a, still some 13DB molecules are adsorbed with "S" geometry (highlighted by white arrows) on the surface. As a result, no distinct boundary between "R" and "S" domains appears in the SAMs of 13DB. Instead, 13DB molecules adsorbed on the Au(111) surface with mixed "R" and "S" geometry are frequently observed, as demonstrated in Figure 4b. Lamellae of 13DB adsorbed on the Au(111) with identical geometry are marked by minus sign (−) at the bottom of the image, whereas stars (*) mark the lamellae containing both "R" and "S" geometry. Detailed packing of lamellae with mixed "R" and "S" geometry is presented in Figure 4c. As for adjacent 13DB with "R" and "S" geometry, 13DB molecules have been slightly tilted to fit the transition from one enantiomer to the other. Considering the separate "R" and "S" domains in the 12DB SAMs (see Figure 1b), the obvious difference in the 13DB SAMs can be attributed to the so-called "odd−even effect", which is frequently observed in the SAMs of molecules containing alkyl chains.[12] Due to the terminal direction of methyl groups, molecules with an odd carbon number of alkyl chains tend to form different structures in comparison to the

DOI: 10.1021/jacs.6b05597
J. Am. Chem. Soc. 2016, 138, 11743−11748

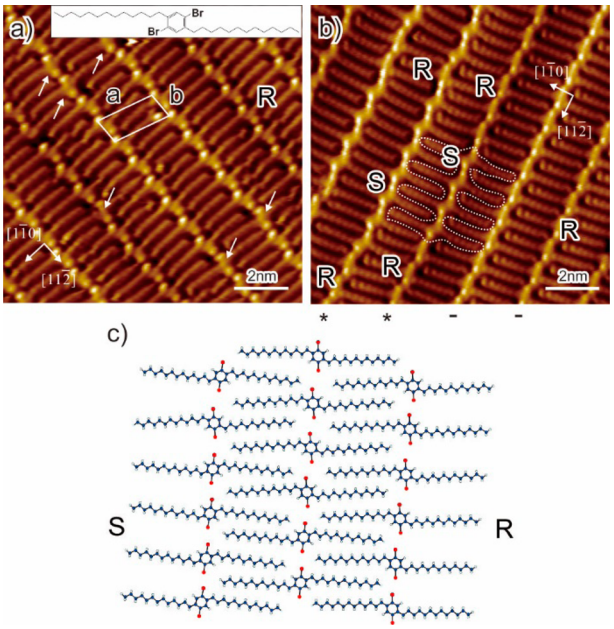

Figure 4. Self-assembled monolayers of 13DB on reconstructed Au(111) surface. (a) 13DB SAMs with dominant "R" structure. Still some 13DB molecules adsorbed with "S" geometry are mixed in the "R" domain, as highlighted by white arrows. Unlike the SAMs of 12DB, homochiral domains can hardly be observed in the 13DB SAMs. (b) 13DB SAMs with mixed "R" and "S" structures. A minus sign (−) at the bottom of the image marks a row of 13DB molecules adsorbed with identical geometry, and a star (*) marks a row of molecules adsorbed with mixed "R" and "S" geometry. (c) Structural model showing detailed packing of lamellae with mixed "R" and "S" geometry.

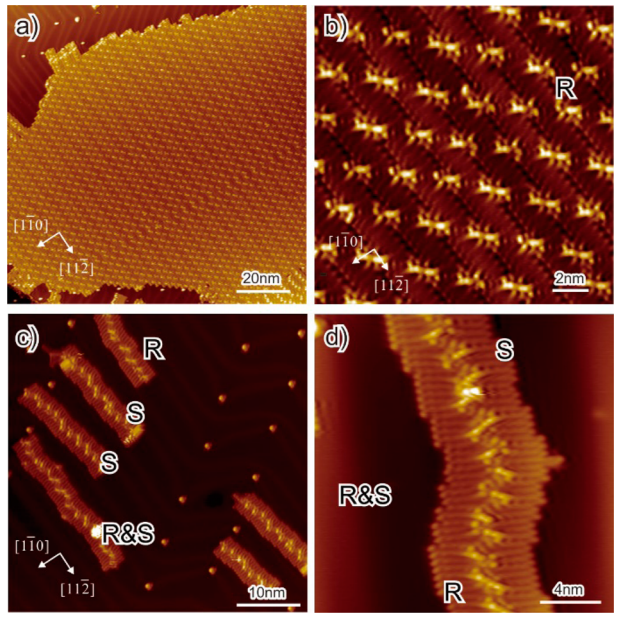

Figure 5. Chirality expression of oligomers from 13DB upon annealing samples of 13DB SAMs at 120 °C. (a) Large-scale STM image of a homochiral domain of 13DB oligomers. (b) Closer view of the homochiral domain with "R" geometry of 13DB oligomers. (c) Separated lamellae of 13DB oligomers showing homochiral and racemic geometry. (d) Closer view of a racemic lamella.

corresponding molecules with an even carbon number within the alkyl chains.[12,17,37] Increasing alkyl chain length with only one single methylene unit can lead to morphology switches from a 2D racemate to a 2D conglomerate at a liquid/substrate interface.[12,37]

To investigate the chirality transfer of the 13DB SAMs, the Au(111) substrate covered by 13DB SAMs was annealed at 120 °C for on-surface coupling reactions. New packing structures are observed in the SAMs of 13DB OPP (Figure 5a), showing a large-scale domain with identical chirality. A magnified STM image of the domain (see Figure 5b) displays detailed packing of 13DB OPP. A staggered packing structure, in addition to lamellar structure, can be distinguished from the SAMs of 13DB oligomers, which has rarely been observed in the 2D packing of oligophenylene obtained from 12DB. We attribute the change in packing of 13DB OPP to the increased alkyl chain length. The longer alkyl chain can slightly increase the adsorption energy of 13DB (about 12.4 kJ/mol),[38] which, in turn, affects the reaction of 13DB. A higher adsorption energy of 13DB might impede the squeezing process in adjacent lamellae, leading to the staggered packing of 13DB oligomers.

Recalling that no homochiral domains are observed in the 13DB SAMs, the "R" domain of 13DB OPP should be formed from "R"-dominated SAMs. We guess that a few 13DB molecules with "S" geometry are squeezed out from the "R"-dominated domain during the on-surface coupling reaction. However, in domains with mixed "R" and "S" 13DB lamellae, annealing of the SAMs at 120 °C gives rise to the formation of separated lamellae with either identical or mixed chirality, as depicted in Figure 5c. The detailed structure of a mixed lamellae can be seen in Figure 5d, in which 13DB OPP with "R" and "S" adsorption geometry are close-packed to form a blend lamella due to the symmetry plane between "R" and "S" geometry. Since such a racemic lamella has never been obtained from 12DB SAMs, its formation reveals the structural correlation between the SAMs and the produced OPP.

Chirality transfer from self-assembled 12(13)DB precursors to OPP via on-surface synthesis should proceed several steps, such as breaking of active bonds, coupling of adjacent radicals, and the self-assembly of OPP. In these processes, the formation and subsequent self-assembly of OPP are critical in chirality transfer and magnification by forming 2D homochiral domains. In the aryl−aryl coupling of 12(13)DB precursors, only short OPP_n (where n is the number of phenylene moieties), such as OPP_3 and OPP_4, are synthesized on Au(111) surfaces (ca. 120 °C), which facilitate the self-assembly process to form well-ordered 2D homochiral domains on surfaces. Careful inspection of the structure of 12(13)DB OPP reveals that alkyl chains of OPP are adsorbed along the [1$\bar{1}$0] direction (Figures 2b, 3a,c, and 5b,c). The intramolecular distance between alkyl chains is measured to be 0.49 ± 0.01 nm (averaged with more than tens of STM images). The measured distance (0.49 nm) equals the periodic distance of gold atoms along the [11$\bar{2}$] direction (0.5 nm). Recalling that normal alkanes are adsorbed on gold atom troughs along ⟨110⟩ directions to form commensurate structures on reconstructed Au(111) surfaces,[17] we assume that the adsorption geometry of OPP is essentially to optimize adsorbate−substrate interactions on Au(111). It is therefore safe to claim that the self-assembly of OPP should be directed by physical interactions between OPP and Au(111) substrate rather than the covalent bonds between phenylene moieties. Otherwise, random distributions of OPP wires would be expected, similar to the on-surface synthesis of 1D structures.[31−34] Accordingly, a schematic illustration of chirality transfer via on surface reaction of

DOI: 10.1021/jacs.6b05597
J. Am. Chem. Soc. 2016, 138, 11743−11748

12DB is displayed in Figure 6. Molecules marked in green are considered to desorb from the SAMs during parallel connection

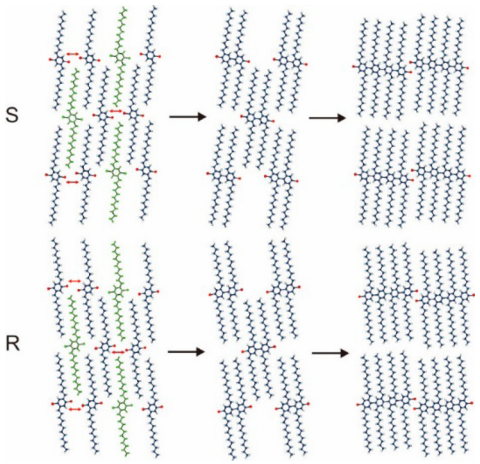

Figure 6. Schematic illustration of chirality transfer from self-assembled 12DB to OPP_4 via on surface synthesis. 12DB precursors marked as green are considered to desorb from self-assembled lamellae for the parallel aryl−aryl coupling of adjacent molecules (indicated by red arrows).

(red arrows) of the nearest neighboring 12DB precursors, as the newly formed C−C bonds can significantly decrease the intermolecular distance of coupled precursors. Interestingly, the intramolecular distance (0.49 nm) between alkyl chains of produced OPP equals the intermolecular distance of alkyl chains in self-assembled lamellar structures, keeping the same physical interactions between alkyl chains during the whole aryl−aryl coupling process. Such an unchanged interaction could account for the chirality transfer from the SAMs to the oligophenylene products because the basic lamellar structures are preserved during the aryl−aryl coupling process with the help of alkyl chains.

CONCLUSION

In summary, we demonstrate that chirality can be transferred from self-assembled 12(13)DB molecules to oligo-*p*-phenylenes via on-surface synthesis. Alkyl chains play a critical role in the controlled coupling reaction of 12(13)DB precursors. Optimized adsorbate−substrate interactions are observed during the whole process of the coupling reaction, preserving the self-assembled lamellar structures and allowing the chirality transfer. Structures of the SAMs can determine the chirality expression of the newly formed oligomers. The strategy developed here sheds new light on the synthesis of stable, structure-adjustable chiral surfaces from 2D molecular self-assembly. Although produced OPP oligomers appear with chiral characteristics only when they are confined on surfaces, the method can be readily applied to the synthesis of 1D functional polymers with "planar chirality", for example, chiral graphene nanoribbons. Furthermore, a homochiral surface with enhanced stability can be expected in combination with the techniques for the preparation of pure 2D homochiral surfaces[18−20] and the concept for chirality transfer present in this work.

ASSOCIATED CONTENT

Supporting Information

The Supporting Information is available free of charge on the ACS Publications website at DOI: 10.1021/jacs.6b05597.

Experimental details, STM image of the sample annealed at 160 °C, and synthesis of 12(13) DB (PDF)

AUTHOR INFORMATION

Corresponding Author

*chilf@suda.edu.cn

Notes

The authors declare no competing financial interest.

ACKNOWLEDGMENTS

This work was supported by the National Natural Science Foundation of China (NSFC, Grant Nos. 91227201 and 21527805). We also thank the Collaborative Innovation Center of Suzhou Nano Science & Technology, and the Priority Academic Program Development of Jiangsu Higher Education Institutions. K.M. acknowledges support from the Johannes Gutenberg University via a Gutenberg Research Fellowship.

REFERENCES

(1) Seo, J. S.; Whang, D.; Lee, H.; Jun, S. I.; Oh, J.; Jeon, Y. J.; Kim, K. *Nature* **2000**, *404*, 982.
(2) Noyori, R. *Angew. Chem., Int. Ed.* **2002**, *41*, 2008.
(3) Wu, C. D.; Hu, A.; Zhang, L.; Lin, W. *J. Am. Chem. Soc.* **2005**, *127*, 8940.
(4) Lopinski, G. P.; Moffatt, D. J.; Wayner, D. D. M.; Wolkow, R. A. *Nature* **1998**, *392*, 909.
(5) Ernst, K. H. *Phys. Status Solidi B* **2012**, *249*, 2057.
(6) Elemans, J. A. A. W.; De Cat, I.; Xu, H.; De Feyter, S. *Chem. Soc. Rev.* **2009**, *38*, 722.
(7) Mu, Z. C.; Shu, L. J.; Fuchs, H.; Mayor, M.; Chi, L. F. *J. Am. Chem. Soc.* **2008**, *130*, 10840.
(8) Ortega Lorenzo, M.; Baddeley, C. J.; Muryn, C.; Raval, R. *Nature* **2000**, *404*, 376.
(9) Kühnle, A.; Linderoth, T. R.; Hammer, B.; Besenbacher, F. *Nature* **2002**, *415*, 891.
(10) Yuan, Q. H.; Yan, C. J.; Yan, H. J.; Wan, L. J.; Northrop, B. H.; Jude, H.; Stang, P. J. *J. Am. Chem. Soc.* **2008**, *130*, 8878.
(11) Weckesser, J.; De Vita, A.; Barth, J. V.; Cai, C.; Kern, K. *Phys. Rev. Lett.* **2001**, *87*, 096101.
(12) Wei, Y. H.; Kannappan, K.; Flynn, G. W.; Zimmt, M. B. *J. Am. Chem. Soc.* **2004**, *126*, 5318.
(13) Vidal, F.; Delvigne, E.; Stepanow, S.; Lin, N.; Barth, J. V.; Kern, K. *J. Am. Chem. Soc.* **2005**, *127*, 10101.
(14) Zhang, J.; Li, B.; Cui, X. F.; Wang, B.; Yang, J. L.; Hou, J. G. *J. Am. Chem. Soc.* **2009**, *131*, 5885.
(15) De Feyter, S.; Grim, P. C. M.; Rücker, M.; Vanoppen, P.; Meiners, C.; Sieffert, M.; Valiyaveettil, S.; Müllen, K.; De Schryver, F. C. *Angew. Chem., Int. Ed.* **1998**, *37*, 1223.
(16) Schöck, M.; Otero, R.; Stojkovic, S.; Hümmelink, F.; Gourdon, A.; Lægsgaard, E.; Stensgaard, I.; Joachim, C.; Besenbacher, F. *J. Phys. Chem. B* **2006**, *110*, 12835.
(17) Zhang, H. M.; Xie, Z. X.; Mao, B. W.; Xu, X. *Chem. - Eur. J.* **2004**, *10*, 1415.
(18) Parschau, M.; Romer, S.; Ernst, K. H. *J. Am. Chem. Soc.* **2004**, *126*, 15398.
(19) Masini, F.; Kalashnyk, N.; Knudsen, M. M.; Cramer, J. R.; Lægsgaard, E.; Besenbacher, F.; Gothelf, K. V.; Linderoth, T. R. *J. Am. Chem. Soc.* **2011**, *133*, 13910.
(20) Tahara, K.; Yamaga, H.; Ghijsens, E.; Inukai, K.; Adisoejoso, J.; Blunt, M. O.; De Feyter, S.; Tobe, Y. *Nat. Chem.* **2011**, *3*, 714.
(21) Grill, L.; Dyer, M.; Lafferentz, L.; Persson, M.; Peters, M. V.; Hecht, S. *Nat. Nanotechnol.* **2007**, *2*, 687.
(22) Weigelt, S.; Busse, C.; Bombis, C.; Knudsen, M. M.; Gothelf, K. V.; Lægsgaard, E.; Besenbacher, F.; Linderoth, T. R. *Angew. Chem., Int. Ed.* **2008**, *47*, 4406.

DOI: 10.1021/jacs.6b05597
J. Am. Chem. Soc. 2016, 138, 11743−11748

(23) Haq, S.; Hanke, F.; Dyer, M. S.; Persson, M.; Iavicoli, P.; Amabilino, D. B.; Raval, R. *J. Am. Chem. Soc.* **2011**, *133*, 12031.
(24) Lipton-Duffin, J. A.; Ivasenko, O.; Perepichka, D. F.; Rosei, F. *Small* **2009**, *5*, 592.
(25) Bieri, M.; Nguyen, M. T.; Gröning, O.; Cai, J. M.; Treier, M.; Ält-Mansour, K.; Ruffieux, P.; Pignedoli, C. A.; Passerone, D.; Kastler, M.; Müllen, K.; Fasel, R. *J. Am. Chem. Soc.* **2010**, *132*, 16669.
(26) Zhang, Y. Q.; Kepcija, N.; Kleinschrodt, M.; Diller, K.; Fischer, S.; Papageorgiou, A. C.; Allegretti, F.; Bjork, J.; Klyatskaya, S.; Klappenberger, F. *Nat. Commun.* **2012**, *3*, 1286.
(27) Gao, H. Y.; Wagner, H.; Zhong, D. Y.; Franke, J.; Studer, A.; Fuchs, H. *Angew. Chem., Int. Ed.* **2013**, *52*, 4024.
(28) Zwaneveld, N. A. A.; Pawlak, R.; Abel, M.; Catalin, D.; Gigmes, D.; Bertin, D.; Porte, L. *J. Am. Chem. Soc.* **2008**, *130*, 6678.
(29) Dienstmaier, J. F.; Gigler, A. M.; Goetz, A. J.; Knochel, P.; Bein, T.; Lyapin, A.; Reichlmaier, S.; Heckl, W. M.; Lackinger, M. *ACS Nano* **2011**, *5*, 9737.
(30) Wang, W. H.; Shi, X. Q.; Wang, S. Y.; Van Hove, M. A.; Lin, N. *J. Am. Chem. Soc.* **2011**, *133*, 13264.
(31) Zhang, H. M.; Lin, H. P.; Sun, K. W.; Chen, L.; Zagranyarski, Y.; Aghdassi, N.; Duhm, S.; Li, Q.; Zhong, D. Y.; Li, Y. Y.; Müllen, K.; Fuchs, H.; Chi, L. F. *J. Am. Chem. Soc.* **2015**, *137*, 4022.
(32) Cai, J. M.; Ruffieux, P.; Jaafar, R.; Bieri, M.; Braun, T.; Blankenburg, S.; Muoth, M.; Seitsonen, A. P.; Saleh, M.; Feng, X. L.; Müllen, K.; Fasel, R. *Nature* **2010**, *466*, 470.
(33) Chen, Y. C.; de Oteyza, D. G.; Pedramrazi, Z.; Chen, C.; Fischer, F. R.; Crommie, M. F. *ACS Nano* **2013**, *7*, 6123.
(34) Basagni, A.; Sedona, F.; Pignedoli, C. A.; Cattelan, M.; Nicolas, L.; Casarin, M.; Sambi, M. *J. Am. Chem. Soc.* **2015**, *137*, 1802.
(35) Grim, P. C. M.; De Feyter, S.; Gesquière, A.; Vanoppen, P.; Rüker, M.; Valiyaveettil, S.; Moessner, G.; Müllen, K.; De Schryver, F. C. *Angew. Chem., Int. Ed. Engl.* **1997**, *36*, 2601.
(36) Banerjee, M.; Shukla, R.; Rathore, R. *J. Am. Chem. Soc.* **2009**, *131*, 1780.
(37) Katsonis, N.; Lacaze, E.; Feringa, B. L. *J. Mater. Chem.* **2008**, *18*, 2065.
(38) Wetterer, S. M.; Lavrich, D. J.; Cummings, T.; Bernasek, S. L.; Scoles, G. *J. Phys. Chem. B* **1998**, *102*, 9266.

DOI: 10.1021/jacs.6b05597
J. Am. Chem. Soc. 2016, 138, 11743−11748